

## **Rock physics templates for analysis of brittleness index, mineralogy, and porosity – a Barnett Shale case study**

Z. Guo (British Geological Survey), M. Chapman (University of Edinburgh), X.Y. Li (British Geological Survey)

### **SUMMARY**

Rock brittleness plays a significant role in effective hydraulic fracturing for shale gas production, and is often related to mineralogy, mechanical properties, and microstructure features in shales. We construct a rock physics workflow to link elastic properties of shales to complex constituents and specific microstructure attributes. Multiple compositions and various pore geometries are considered using a self-consistent approximation (SCA) method. The laminated textures due to the preferred orientations of clay particles and possible laminated distribution of kerogen are considered using Backus averaging method to model the anisotropy of shales. Our rock physics model is calibrated on the well log data from the Barnett Shale, and is applied to generate rock physics templates for the interpretation and prediction of shale rock brittleness, mineral constituents, and porosity from elastic properties of shales. Results also show that the lamination of clay particles significantly reduces the sensitivity of shale elastic properties to porosity. Seismic AVO analysis based on the modeling data from top and bottom of the Barnett Shale formation illustrates that AVO intercept and gradient have predictable trends according to the variation of brittleness index, mineralogy, and porosity, which means that we can predict such characterizations from seismic responses.

## Introduction

Complex constituents and specific microstructure attributes in shales have crucial impacts on their mechanical and elastic properties, and therefore on rock brittleness, fluid-flow and seismic-wave propagation. Because rock brittleness plays a significant role in effective hydraulic fracturing for shale gas production, it is important to evaluate and detect rock brittleness from well log data and seismic data. Rock brittleness index is often related to mineralogy, mechanical properties, and microstructure features. In this study, our objective is to construct a rock physics workflow to model shales by considering complexity of constituents and pore geometries using a self-consistent approximation (SCA) method, and modeling the anisotropy resulting from the preferred orientations of clay particles and possible laminated distribution of kerogen using Backus averaging method. We investigate how to detect rock brittleness, mineralogy, and porosity of shales using rock physics templates of different crossplots of elastic properties. The application for the detection of such properties of shales using seismic AVO analysis is illustrated on the reflections from both top and bottom of the Barnett Shale formation.

## Method

The workflow for our shale rock physics model is shown in Figure 1 (a). Though a similar framework can be found in the work of Xu and Payne (2009) for modeling carbonate rocks, this study focuses on a workflow determined by specific characterization of shales. Firstly, we use the SCA method to model shale rocks, considering multiple mineralogical phases, and pores and cracks geometries. Aspect ratio of pore-space is regarded as a random variable following normal distribution (Jiang and Spikes, 2011) with a sample of 100 and specified by mean value and standard deviation. Saturated pores are treated as inclusions of oil/gas/water mixtures. The proportions of clay particles and organic materials of random distribution are also modeled in the first step in Figure 1 (a). In the second step, the factors resulting in the anisotropy of shales are considered. The proportions of clay particles and organic matter with laminated textures are modeled using the Backus averaging method. Schematics in Figure 1 (b) show the microstructure related to preferred orientation of clay particles with different degrees of lamination. The possible presence of bedding-parallel fractures can also be modeled in a straightforward way in this step. Finally, after accounting for the VTI (vertical transverse isotropy) in the shales, many theories can be used to model the possible presence of vertical fractures. In this study, we focus on the VTI anisotropy of shales modeled by the first two steps.

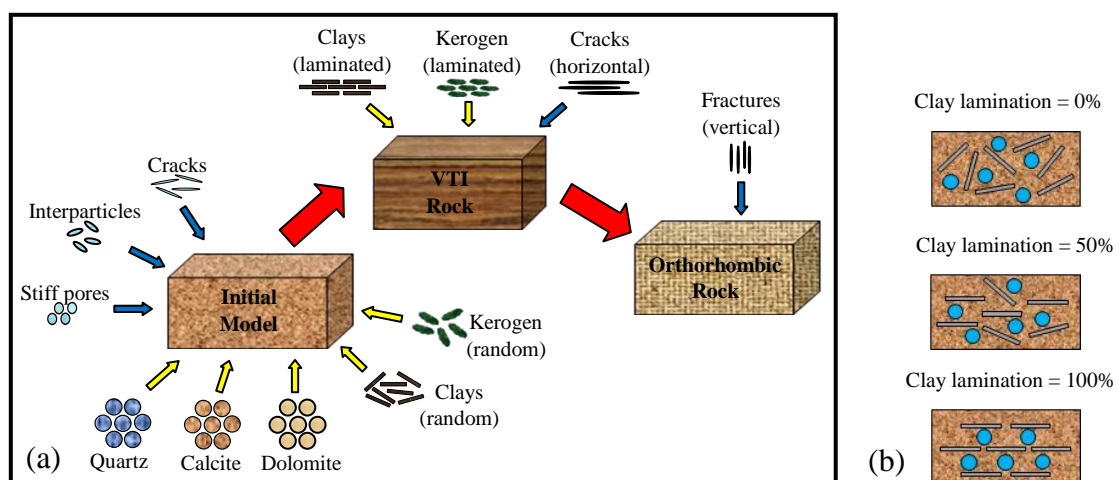


**Figure 1** Diagram of shale rock physics model. (a) Workflow for shale rock physics. (b) Microstructure of preferred orientation of clay particles with different degree of lamination texture.

We construct rock physics templates and analyze the effect of mineralogy and porosity on the elastic properties of shale rocks. Constituents include minerals of quartz, clay, and calcite. The mineral content changes between quartz and clay, while the content of calcite is kept constant. Rock physics

templates in Figure 2 illustrate the mapping of lines of constant porosity and mineralogical mixtures on the crossplots of different elastic properties. Mineral grains and pores in shale rocks are assumed to be randomly distributed, and the aspect ratio of pores is set to 0.1. In Figure 3, the effects of clay particle lamination are shown on the crossplots of Poisson's ratio ( $\nu$ ) and Young's modulus ( $E$ ). An increasing degree of clay lamination decreases  $E$  and increases  $\nu$ , making shale rocks more ductile. An increasing degree of clay lamination also reduces the sensitivity of  $E$  and  $\nu$  to porosity, especially for high clay content. Such an impact is most significant for the case of 100% clay lamination and 80% clay content, as shown in Figure 3 (c).

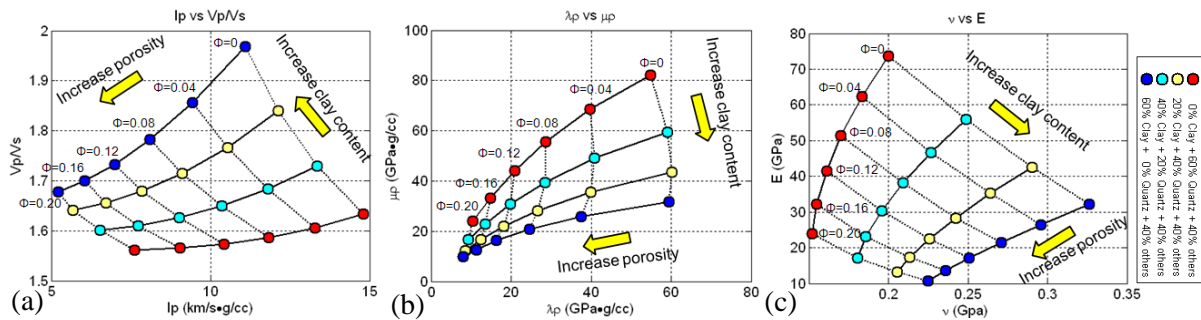


**Figure 2** Rock physics templates showing the effect of mineralogical mixtures and porosity on the crossplots of (a)  $I_p$  versus  $V_p/V_s$ , (b)  $\lambda\rho$  versus  $\mu\rho$ , and (c)  $\nu$  versus  $E$ .

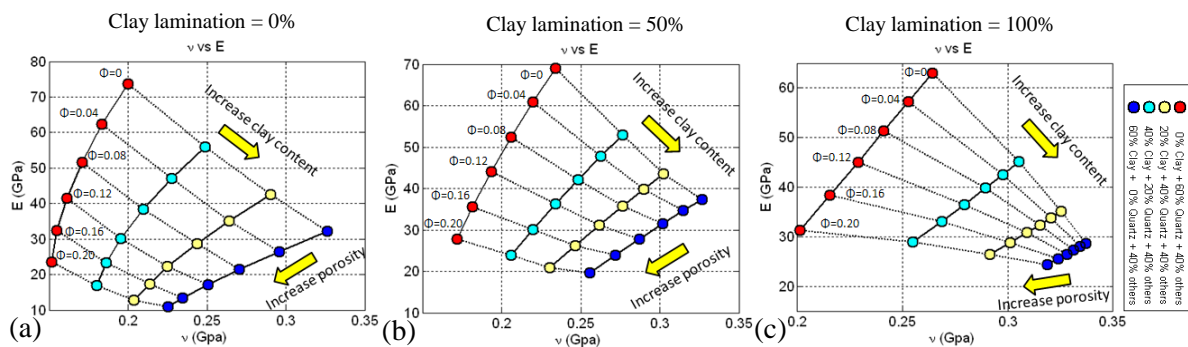


**Figure 3** Crossplots of Poisson's ratio ( $\nu$ ) versus Young's modulus ( $E$ ) showing the effect of the degree of clay particles lamination. (a) 0%, (b) 50%, and (c) 100%.

## Examples

Figure 4 (a) shows mineralogical volume fractions from core samples of the Barnett Shale. The mineralogical content has a large variation, with a dominant content of quartz and clay in the rocks. The ternary plot in Figure 4 (b) shows the content of quartz varies from around 20% to 60%, and that of clay from about 5% to 40%.

We calibrate our shale rock physics model on well log data by crossplots of  $I_p$  versus  $V_p/V_s$  in Figure 5 (a) and (b) constructed using our shale rock physics model. The average value of aspect ratio is set to 0.1, and clay-related porosity is assumed to be 20% of the total porosity. The degree of clay lamination is set to 100% as it gives the best fit to the well log data of the study. The spreads of data points are within the range of mineralogical content and porosity displayed in volumetric fractions in Figure 4 and well log in Figure 6 (d), which shows the ability of our model to describe the real data. Further work may include the inversion of porosity and mineralogy based on the templates for detailed analysis.

Rock brittleness, defined in two different ways, is calculated and colour-coded on the templates in Figure 5 (a) and (b). Rickman et al. (2008) believe that higher Young's modulus ( $E$ ) and lower Poisson's ratio ( $\nu$ ) correspond to rocks with greater brittleness, so we propose to use the index in

Equation (1) as a measure of rock brittleness. The other way to estimate rock brittleness is proposed by Goodway et al. (2010) who believe that the most fracable zones occupy low  $\lambda\rho$  and midrange  $\mu\rho$ . We use a modified version of their definition as a brittleness index as shown in Equation (2).

$$\text{Brittleness\_index} = \frac{E}{\nu} \quad (1)$$

$$\text{Brittleness\_index} = \frac{\lambda + 2\mu}{\lambda} \quad (2)$$

We can observe from Figure 5 that increasing clay content will decrease brittleness index, while difference exists between these two definitions on the constant porosity lines. The highest value of brittleness index given by  $\lambda-\mu$  occurs at 20% porosity, while the value defined by E-v is at zero porosity. Meanings of brittleness index defined by various elastic parameters deserve further study.

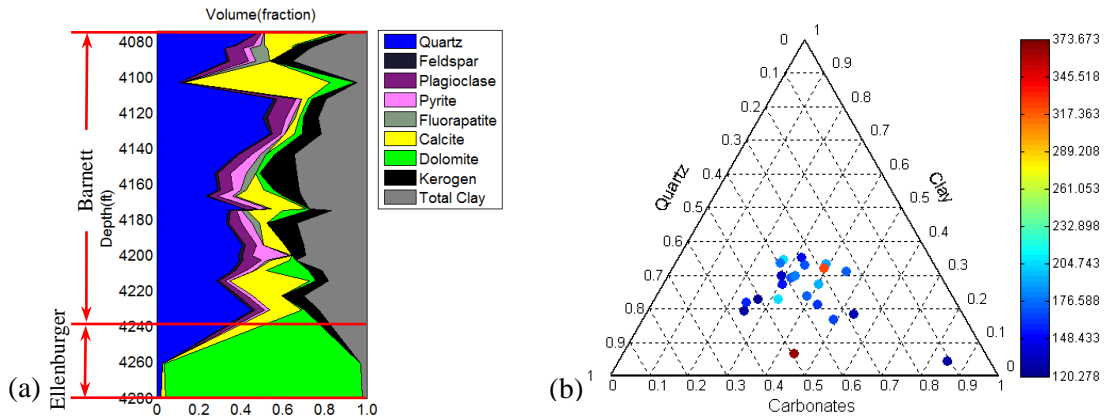


**Figure 4** Mineralogy of the Barnett Shale. (a) Mineral volume fraction. (b) Ternary plot of mineral compositions of the Barnett Shale, colour coded by gamma ray values.

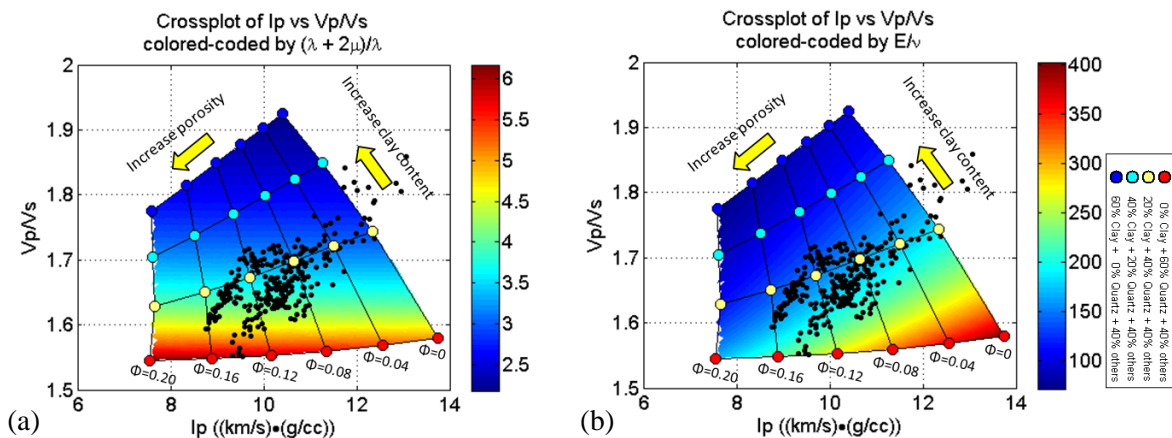


**Figure 5** Shale rock physics templates of  $I_p$  versus  $V_p/V_s$ , showing the effect of mineralogy, porosity, and brittleness index. The templates are colour-coded by (a)  $(\lambda + 2\mu)/\lambda$ , and (b)  $E/\nu$  respectively to show the brittleness index of shale rocks.

Well logs of the Barnett Shale and surrounding formations are illustrated in Figure 6. Data points of  $V_p/V_s$  and porosity from the well logs are superimposed on the templates in Figure 5. Analysis shows that the templates describe the data points reasonably. Clay content as indicated by the templates has a spread from zero to around 20%, and porosity from zero to about 16%, which is consistent with the mineralogical analysis in Figure 4 and well log data in Figure 6. Future work may include inversion of clay content, porosity, and brittleness index using the constructed rock physics templates in Figure 5.

In Figure 7, seismic AVO responses of P-P waves reflected from both top and bottom of the Barnett Shale are calculated, and the corresponding results are shown on the AVO intercept and gradient crossplot with constant porosity and mineralogy lines, colour-coded by rock brittleness index defined by E and v. The trend on the crossplot of AVO intercept and gradient shows predictable variations

according to mineralogical contents, porosity, and brittleness index of the Barnett Shale, which means we can use seismic AVO for the prediction of such rock properties.

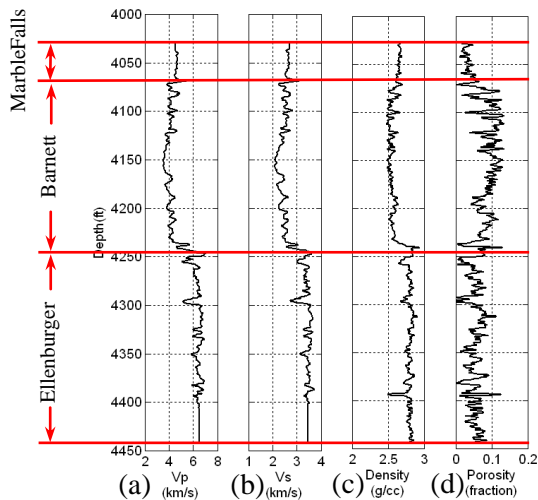


**Figure 6** Well logs for the formations of Marble Falls, Barnett, and Ellenburger, showing (a) P-wave velocity, (b) S-wave velocity, (c) density, and (d) porosity.

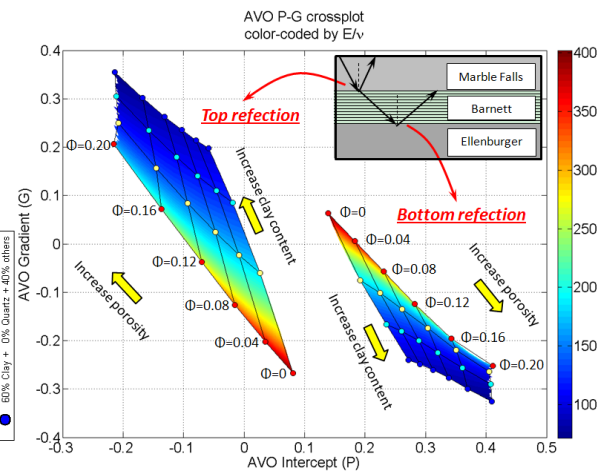


**Figure 7** Seismic AVO intercept-gradient crossplot coloured-code by brittleness index, showing the effect of mineralogical mixtures and porosity.

## Conclusions

A rock physics workflow is constructed to model complexity of constituents and pore geometries in shales using the SCA method. Anisotropy resulting from preferable orientation of clays and possible laminated distribution of organic materials is modeled using the Backus averaging method. The results from our rock physics model are calibrated on the well log data, and rock physics templates based on the model show that we can predict rock brittleness index, mineralogy, and porosity from crossplots of elastic properties. Seismic AVO analysis based on the modeling data from top and bottom of the Barnett Shale formation illustrates that AVO intercept and gradient have predictable trends according to the variation of brittleness index, mineralogy, and porosity, which provides another way characterize the Barnett Shale. Results also show that the lamination of clay particles significantly reduces the sensitivity of shale elastic properties to porosity.

## Acknowledgements

The work is presented with the permission of the EAP Sponsors and the Executive Director of British Geological Survey (NERC).

## References

- Goodway, B., Perez, M., Varsek, J. and Abaco, C. [2010] Seismic petrophysics and isotropic-anisotropic AVO methods for unconventional gas exploration. *The Leading Edge*, **29**(12), 1500-1580.
- Jiang, M. and Spikes, K.T. [2011] Pore-shape and composition effects on rock-physics modeling in the Haynesville Shale. *81th Annual International Meeting, SEG, Expanded Abstracts*, 2079-2083.
- Rickman, R., Mullen, M., Petre, E., Grieser, B. and Kundert, D. [2008] A practical use of shale petrophysics for simulation design optimization: All Shale plays are not clones of the Barnett Shale. *SEP*, 115258.
- Xu, S. and Payne, M.A. [2009] Modeling elastic properties in carbonate rocks. *The Leading Edge*, **28**(1), 66-74.